DOI: 10.1002/marc.((insert number))

Article Type: Communication

Light-driven, caterpillar-inspired miniature inching robot[a]

Hao Zeng*, Owies M. Wani, Piotr Wasylczyk, Arri Priimagi*

Dr. H. Z., O. M., Prof. A. P.
Laboratory of Chemistry and Bioengineering, Tampere University of Technology, P.O. Box 541, FI 33101 Tampere, Finland
E-mail: hao.zeng@tut.fi, arri.priimagi@tut.fi

Dr. P. W.
Photonic Nanostructure Facility, Institute of Experimental Physics, Faculty of Physics, University of Warsaw, ul. Pasteura 5, 02-093 Warsaw, Poland

Keywords: biomimetic; liquid crystal elastomer; locomotion; photoactuation; azobenzene

Abstract: Liquid crystal elastomers are among the best candidates for artificial muscles, and the materials of choice when constructing micro-scale robotic systems. Recently, significant efforts have been dedicated to designing stimuli-responsive actuators that can reproduce the shape-change of soft bodies of animals by means of proper external energy source. However, transferring material deformation efficiently into autonomous robotic locomotion remains a challenge. This paper reports on a miniature inching robot fabricated from a monolithic liquid crystal elastomer film, which upon visible-light excitation is capable of mimicking caterpillar locomotion on different substrates like a blazed grating and a paper surface. The motion is driven by spatially uniform visible light with relatively low intensity, rendering the robot "human-friendly", *i.e.*, operational also on human skin. The design paves way towards light-driven soft, mobile micro-devices capable of operating in various environments, including the close proximity of humans.

[a] **Supporting Information** is available online from the Wiley Online Library or from the author.

1. Introduction

Liquid crystal elastomers (LCEs) are smart, artificial-muscle-like materials that can be used to devise remotely-controlled actuators and miniaturized robotic systems.[1-3] LCEs consist of liquid-crystal monomers chemically bonded to a low-crosslink-density polymer network, forming a flexible elastomer that maintains a pre-designed distribution of molecular directors.[4-6] By incorporating light-responsive molecules into the polymer network, the molecular alignment can be controlled with an external light field. The light response can be either photochemical or photothermal in nature, triggering reversible photomechanical actuation in the macroscopic scale and generating stress comparable to the one of human muscle.[7,8] Multitude of versatile chemical approaches towards LCE design exist,[9-11] and several techniques to control the molecular alignment have been developed.[12-14] By combining these technologies, several sophisticated photoactuation schemes have been reported recently.[15-17] In particular, bioinspired light-driven actuators such as artificial cilia,[18] polymeric strips mimicking plant twist and seedpod opening,[19,20] and light-driven flytrap mimic,[21] have been developed.

Realization of photomobile LCE devices requires a strategy to transfer photomechanical deformation into locomotion, which still poses a challenge in LCE soft robotics. Different from micro-devices driven by magnetic fields,[22,23] the light-responsive LCE robots are not driven by external forces or torques, hence the locomotion is totally determined by the interaction between the robot body and its environment. At small length scales (few millimeters or less) the ratio between different forces involved (light-driven elastic force, adhesion/friction, inertial force) become dramatically different from those observed in human-scale machines, and therefore the locomotion mechanics paradigms need to be revisited.[24] A miniature-sized robot has a small mass, resulting in limited inertia, hence the motion is dominated by forces related to the surfaces, such as adhesion, friction, or drag.[25] Strongly influenced by the environment,

the generation of unidirectional motion is difficult due to limited possibilities for controlling friction between different body parts and the surrounding media. Few light responsive LCE-based walking devices have been reported up to date, in which rigid segments are used to reduce the friction,[26] while additional asymmetric surface is required to create movement tendency.[27,28] Recently, we have developed a crawling LCE robot that can mimic caterpillar deformation upon spatially-modulated illumination (a scanned laser beam).[29] All the earlier approaches have been based on illumination with either UV light or high-intensity (> 10 W cm^{-2}) visible or infrared light to generate the movement. However, future foreseeable applications in biomedicine, human–robot interactions, or entertainment, call for human-friendly micro-robots, *i.e.*, devices that can operate under conditions that pose no hazard to the operator/user even when in close proximity of human body.

Here, we report a novel method to fabricate an LCE robot that mimics the inching locomotion of caterpillar under illumination with spatially uniform visible light. The robot is made of monolithic LCE actuator, composed of three segments with engineered splayed orientation. The segments adapt a caterpillar-like deformation geometry due to bending induced by anisotropic thermal expansion (**Figure 1**). The robot can be actuated with visible light with moderate intensity, providing human-safe operation, and performing inching movements without spatial control of the light beam. The robot can sense the ground surface condition and perform different gait modes, as demonstrated by movement on a series of substrates, such as blazed grating, paper surface and human skin.

2. Experimental Section

2.1 Design strategy

Inching is a common locomotion strategy adapted by caterpillars.[30] As shown in Figure 1a, during the motion cycle the front legs (thoracic legs) act as anchors and grip to the ground,

while the middle part of the body is lifted up, deforming the body into a "Ω"-like shape. Then, the caterpillar switches onto its posterior legs (terminal prolegs) to hold the ground, detaches its front legs, and extends the body into a linear shape. This motion cycle allows transferring the body deformation into one step length, and the net motion enables the caterpillar to efficiently navigate around obstacles. To mimic the inching deformation, we use a single strip made of light-responsive LCE with carefully designed alignment distribution. As shown in Figure 1b, the strip contains three alternating splay-aligned segments, each deforming into an arc, that together give rise to a "Ω"-like geometry of the robot soft body. The fact that the robot adapts such shape even without light irradiation is enabled by anisotropic thermal expansion that is generated by photopolymerization at elevated temperatures.[31] Upon light illumination, the absorbed light energy is transferred into heat inside the LCE, making the curved structure to become flat, and resulting in extension of the body. When the light is switched off, heat releases to the environment, and the robot retains its original shape. As the photomechanical actuation is reversible, the robot can perform cyclic deformation by simply switching on and off the light source, thereby mimicking the inching gait. Due to the reciprocal nature of the actuation cycle, the walking tendency of the robot is influenced by the friction bias induced by the contact surface, and possibly also by asymmetric defects created during the robot fabrication. During light actuation, the inching robot keeps slipping between the two legs and senses the surface topology, which leads to different performance on different surfaces.

2.2 Fabrication

A glass slide was first spin coated with polyvinyl alcohol (PVA, 1 wt% water solution, 4000 RPM, 1 min) and rubbed unidirectionally (**Figure 2**a). Then the rubbed PVA layer was covered by Teflon adhesive tape, leaving a 4 mm wide opening in the direction perpendicular to the rubbing (Figure 2b). Another layer, giving rise to homeotropic molecular alignment (JSR OPTMER), was then spin coated (6000 RPM, 1 min) onto the PVA-coated slide (partially

covered with tape). After the second spin coating, the tape was removed, leading to an alignment layer with three distinct domains: homeotropic in the center, and rubbed at the edges (Figure 2c). A baking process (100 °C for 10 min, 160 °C for 30 min) was applied to stabilize the homeotropic layer. Another glass slide was prepared using the same technique but in the negative, such that the edges contained the homeotropic alignment layer and the central area was rubbed (Figure 2d). An LC cell was formed by combining these two glass slides, using 10 μm spacers between them and carefully aligning the central areas with homeotropic/rubbed alignment layers on the two slides. Liquid-crystal monomer mixture was then infiltrated into the cell in a temperature where the mixture was isotropic (70 °C), and cooled down to 45 °C (5 °C per min) to reach a nematic phase with splayed molecular alignment. The alignment distribution across the different regions is illustrated in Figure 2e. We used commercially available acrylate-functionalized LC monomers and cross-linkers (Figure 2f) to form the polymer network, photo-initiator (2,2-Dimethoxy-2-phenylacetophenone, Sigma Aldrich) and Disperse Red 1 doped into the polymer network as a light-responsive unit.[21] A UV lamp (Prior Scientific; 150 mW cm^{-2}, 385 nm, 1 min) was used to polymerize the mixture at 45 °C. The polymerized LCE exhibited a glass transition in the temperature range 0-20 °C,[31] and the nematic-to-isotropic phase transition temperature, determined with a polarized-optical microscope, was above 200 °C.

After cooling to room temperature (T_R), a 2 mm wide strip was cut from the film, such that it contained the three alignment sections within the length of 14 mm. Due to significant difference between polymerization temperature (45 °C) and operation temperature (T_R = 22 °C), anisotropic thermal expansion of the LCE[31-33] induced different stresses between the two surfaces of the film. After releasing these stresses by annealing at 50 °C, the strip spontaneously deformed into the desired "Ω"-like shape, as shown in Figure 2g. This spontaneous, anisotropic thermal expansion -induced bending is in the opposite direction than the light-induced bending, and upon light illumination, the strip straightened out and adapted a flat shape (Figure 2h).

Cycling the actuator between the curled and flat stages can be achieved by turning on and off a light source, thereby providing the mechanism for the robot control.

3. Results and Discussion

3.1. Photomechanical actuation

To analyse the photomechanical action of the inching robot, we measured the change in body length upon different irradiation intensities. To characterize the deformation without influence of friction from the substrate, we attached the central part of the body of the robot to a fiber tip (insets in **Figure 3**a). A spatially filtered, continuous-wave laser beam (488 nm) with a diameter of 15 mm was projected on the top of the strip, and the shape change was monitored with a side-view camera. As shown in Figure 3a, by increasing the light intensity, the "Ω"-shaped body extended into a flat shape at around 120 mW cm^{-2}, corresponding to body length change from 8 mm to 13 mm. By further increasing the light intensity, the strip bent in the opposite direction, adapting a reversed geometry accompanied with a decrease in the body length. **Movie 1** in Supporting Information shows an example of such light-induced "Ω" → flat → reversed-"Ω" cycle. The response time of the inching robot depends on the light intensity, as shown in Figure 3b, and at around 200 mW cm^{-2}, the strip completes its shape change within 0.7 s. The photodeformation is mainly caused by light-induced heating, as confirmed by the infrared camera video shown in **Movie 2** (Supporting Information). Upon 130 mW cm^{-2} illumination, the shape change of the LCE is accompanied by the temperature increase from RT to 47 °C. When the irradiation is ceased, the heat releases to the environment, the material cools down, and relaxes back to the original "Ω"-like shape (**Movie 2**). The relaxation takes place at a constant speed of around 2 s, irrespective of the excitation light intensity, as shown in the inset of Figure 3b.

3.2. Light-driven locomotion

A temporally modulated light source (488 nm, 150 mW cm^{-2}, non-polarized, 0.5 Hz) was used to investigate the light-driven locomotion on different surfaces. **Figure 4**a shows the robot performing one stepping cycle on a paper surface. After stepping forward (light on, body extension) and stepping backward (light off, body contraction), it shows a small displacement in the center-of-mass position. When the robot is set on a blazed diffraction grating, the same light excitation leads to significantly larger displacement during one stepping cycle (Figure 4b). The grating (GR50-1208, Thorlabs) consists of 1200 asymmetric grooves per mm, with blaze angle of 26°, and is coated by reflective layer of aluminum. The walking direction is determined by the asymmetric topography of the grating (as indicated in Figure 4b), and even after reversing the robot orientation, it maintained the same walking direction. We recorded the walking distance as a function of time, as shown in Figure 4c, and it is clear that the walking speed is higher on the grating than on the paper surface (see also **Movie 3** in the Supporting Information). Figure 4c also reveals that the moving distance after each inching cycle is different. To study this in more detail, we recorded the length of 66 inching steps on the grating, and 178 steps on the paper surface. The step length distributions for these two cases are presented in Figures 4d and 4e, respectively. Normal distributions are observed in both cases, which indicates that both processes are strongly influenced by randomly distributed friction during the slipping movement. However, inching on the blazed grating has a mean step length of 0.25 mm (corresponding to the walking speed of 0.25 mm s^{-1}) and 0.15 mm on paper (0.15 mm s^{-1}), while the maximum observed step lengths are 2.7 mm on the grating and only 0.8 mm on the paper. The motion on the paper surface also depends on the robot orientation, which we attribute to asymmetry in the robot fabrication process.

Even if some exceptions exist,[34-36] conventional LCE actuation strategies are based on UV-light-induced photochemical reactions, preventing human-friendly interactions. Our approach exploits photothermal heating over a temperature range between 20 and 50 °C under visible-light illumination. Our actuator design combines properly engineered molecular

alignment, and a well-chosen light absorber (Disperse Red 1), allowing us to significantly reduce the light intensity as compared to our previous approach.[29] Thus, the soft robot itself, together with the light source, are totally human-friendly. This is demonstrated in Figure 4f, showing that the robot powered by moderate-intensity visible laser (200 mW cm^{-2}) can perform inching on the nail of a human finger (also see **Movie 4** with movements on human skin).

4. Conclusions

We report a versatile fabrication method to realize millimeter-scale, light-powered inching walker, based on alignment-engineered liquid crystal elastomer film. Photomechanical actuation and locomotion mechanics under spatially uniform illumination have been characterized. The robot can mimic the inching movement of a caterpillar and perform different locomotion on different substrates fueled by visible light at human-safe intensity levels. The combination of LC alignment patterning and visible-light-induced LCE actuation opens up new horizons in photo-mobile devices and human-friendly, small-scale soft robotics.

Supporting Information

Supporting Information is available from the Wiley Online Library or from the author ((delete if necessary))

Acknowledgements: A. P. gratefully acknowledges the financial support of the European Research Council (Starting Grant project PHOTOTUNE; Agreement No. 679646). O. W. is thankful to the graduate school of Tampere University of Technology (TUT), and H. Z. to the TUT postdoctoral fellowship program, for supporting this work.

Received: Month XX, XXXX; Revised: Month XX, XXXX; Published online:

((For PPP, use “Accepted: Month XX, XXXX” instead of “Published online”)); DOI: 10.1002/marc.((insert number)) ((or ppap., mabi., macp., mame., mren., mats.))

Keywords: biomimetic; liquid crystal elastomer; locomotion; photoactuation; azobenzene

References:

1. T. J. White, D. J. Broer, *Nat. Mater.* **2015**, *14*, 1087.

2. S. Palagi, A. G. Mark, S. Y. Reigh, K. Melde, T. Qiu, H. Zeng, C. Parmeggiani, D. Martella, A. Sanchez-Castillo, N. Kapernaum, F. Giesselmann, D. S. Wiersma, E. Lauga, P. Fischer. *Nat. Mater.* **2016**, *15*, 647.

3. H. K. Bisoyi, Q. Li, *Chem. Rev.* **2016**, *116*, 15089.

4. C. Ohm, M. Brehmer, R. Zentel, *Adv. Mater.* **2010**, *22*, 3366.

5. T. Ikeda, J.-i. Mamiya, Y. Yu, *Angew. Chem. Int. Ed.* **2007**, *46*, 506.

6. Intelligent Stimuli-Responsive Materials: From Well-Defined Nanostructures to Applications (Ed: Q. Li), John Wiley & Sons, Hoboken, NJ, USA 2013.

7. J. Naciri, A. Srinivasan, H. Jeon, N. Nikolov, P. Keller, B. R. Ratna, *Macromolecules* **2003**, *36*, 8499.

8. (a) T. Yoshino, M. Kondo, J. Mamiya, M. Kinoshita, Y. Yu, T. Ikeda, *Adv. Mater.* **2010**, *22*, 1361; (b) K. M. Lee, D. H. Wang, H. Koerner, R. A. vaia, L. S. Tan, T. J. White, *Angew. Chem. Int. Ed.* **2012**, *51*, 4117.

9. H. Finkelmann, H.-J. Kock, G. Rehage, Makromol. *Chem., Rapid Commun.* **1981**, *2*, 317.

10. M. Li, P. Keller, B. Li, X. Wang, M. Brunet, *Adv. Mater.* **2003**, *15*, 569.

11. A. Agrawal, A. C. Chipara, Y. Shamoo, P. K. Patra, B. J. Carey, P. M. Ajayan, W. G. Chapman, R. Verduzco, *Nat. Commun.* **2013**, *4*, 1739.

12. T. H. Ware, M. E. McConney, J. J. Wie, V. P. Tondiglia, T. J. White, *Science* **2015**, *347*, 982.

13. H. Zeng, P. Wasylczyk, G. Cerretti, D. Martella, C. Parmeggiani, D. S Wiersma, *Appl. Phys. Lett.* **2015**, *106*, 111902.

14. Y. Xia, G. Cedillo-Servin, R. D. Kamien, S. Yang, *Adv. Mater.* **2016**, *28*, 9637.

15. (a) Y. Yu, M. Nakano, T. Ikeda, *Nature* **2003**, *425*, 145; (b) A. Priimagi, C. J. Barrett, A. Shishido, *J. Mater. Chem. C* **2014**, *2*, 7155.

16. M. E. McConney, A. Martinez, V. P. Tondiglia, K. M. Lee, D. Langley, I. I. Smalyukh, T. J. White, *Adv. Mater.* **2013**, *25*, 5880.

17. L. T. de Haan, V. Gimenez-Pinto, A. Konya, T.-S. Nguyen, J. M. N. Verjans, C. Sánchez-Somolinos, J. V. Selinger, R. L. B. Selinger, D. J. Broer, *Adv. Funct. Mater.* **2014**, *24*, 1251.

18. C. L. van Oosten, C. W. M. Bastiaansen, D. J. Broer, *Nat. Mater.* **2009**, ***8***, 677.

19. S. Iamsaard, S. J. Aßhoff, B. Matt, T. Kudernac, J. J. L. M. Cornelissen, S. P. Fletcher, N. Katsonis, *Nat. Chem.* **2014**, *6*, 229.

20. S. J. Aßhoff, F. Lancia, S. Iamsaard, B. Matt, T. Kudernac, S. P. Fletcher, N. Katsonis, *Angew. Chem. Int. Ed.* **2017**, *56*, 3261.

21. O. M. Wani, H. Zeng, A. Priimagi, *Nat. Commun.* **2017**, DOI: 10.1038/ncomms15546.

22. A. Ghosh, P. Fischer, *Nano Lett.* **2009**, *9*, 2243.

23. D. R. Frutiger, B. E. Kratochvil, K. Vollmers, B. J. Nelson, *IEEE Int. Conf. Robot.* **2008**, 1770.

24. J. J. Wie, M. R. Shankar, T. J. White, Nat. Commun. **2016**, *7*, 13260.

25. E. Diller, M. Sitti, *Found. Trends Databases* **2013**, *2*, 143.

26. H. Zeng, P. Wasylczyk, C. Parmeggiani, D. Martella, M. Burresi, D. S. Wiersma, *Adv. Mater.* **2015**, *27*, 3883.

27. M. Moua, R. R. Kohlmeyer, J. Chen, *Angew. Chem. Int. Ed.* **2013**, *52*, 9234.

28. M. Yamada, M. Kondo, R. Miyasato, Y. Naka, J. Mamiya, M. Kinoshita, A. Shishido, Y. Yu, C. J. Barrett, T. Ikeda, *J. Mater. Chem.* **2009**, *19*, 60.

29. M. Rogoz, H. Zeng, C. Xuan, D. S. Wiersma, P. Wasylczyk, *Adv. Opt. Mater.* **2016**, *4*, 1689.

30. B. A. Trimmer, H. Lin, *Integr. Comp. Biol.* **2014**, *54*, 1122.

31. H. Zeng, O. M. Wani, P. Wasylczyk, R. Kaczmarek, A. Priimagi, *Adv. Mater.* **2017**, in press.

32. K. Urayama, Y. O. Arai, T. Takigawa, *Macromolecules* **2005**, *38*, 3469.

33. D. J. Broer, G. N. Mol, *Polym. Eng. Sci.* **1991**, *31*, 625.

34. Y. Liu, W. Wu, J. Wei, Y. Yu, *ACS Appl. Mater. Interfaces* **2017**, *9*, 782.

35. W. Wu, L. Yao, T. Yang, R. Yin, F. Li, Y. Yu, *J. Am. Chem. Soc.* **2011**, *133*, 15810.

36. K. Kumar, C. Knie, D. Bleger, M. A. Peletier, H. Friedrich, S. Hecht, D. J. Broer, M. G. Debije, A. P. H. J. Schenning, *Nat. Commun.* **2016**, *7*, 11975.

Figure 1. **Inching locomotion in caterpillars and the LCE micro robot.** (a) A caterpillar propels itself by stepping cycles: (i) bending the body, thus forming a "Ω"-like shape, and (ii) then extending the body, thereby transferring the body deformation into one walking step. The scale bar is 1 cm. (b) Our LCE robot mimics the caterpillar inching walking through alternated light actuation: (i) light on → the body extends; (ii) light off → the body bends.

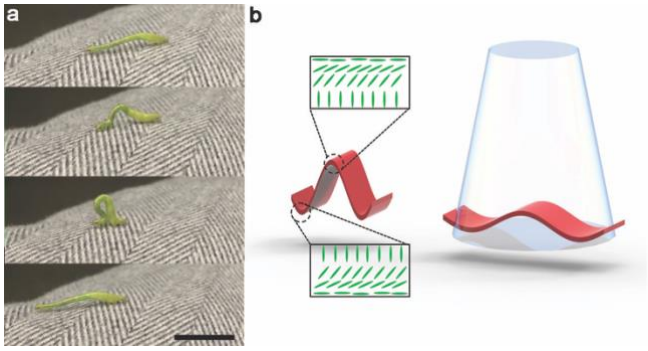

Figure 2. **Alignment patterning and robot fabrication process.** A PVA-coated glass slide is rubbed (a), then covered by a Teflon adhesive tape with a 4 mm-wide-stripe cut from the center (b). Homeotropic alignment layer is spin coated, followed by removal of the Teflon masking tape (c). Another glass slide is made with homeotropic layer covering two edges and rubbed PVA exposed in the middle, then a 10 μm cell is formed by gluing the two slides together (d). The cell is filled with liquid-crystal monomer mixture at 70 °C and then polymerized after cooling to 45 °C. The molecular orientation is schematically shown in (e) and (f) presents the chemical structures of the compounds used. After photo-polymerization, a strip is cut across three patterned alignment regions and detached from the substrate. After releasing the inner stress by annealing, the LCE strip deforms into a caterpillar-mimic, "Ω"-like shape (g), and upon visible light illumination (488 nm, 220 mW cm^{-2}) the LCE robot becomes flat (h). Scale bars: 2 mm.

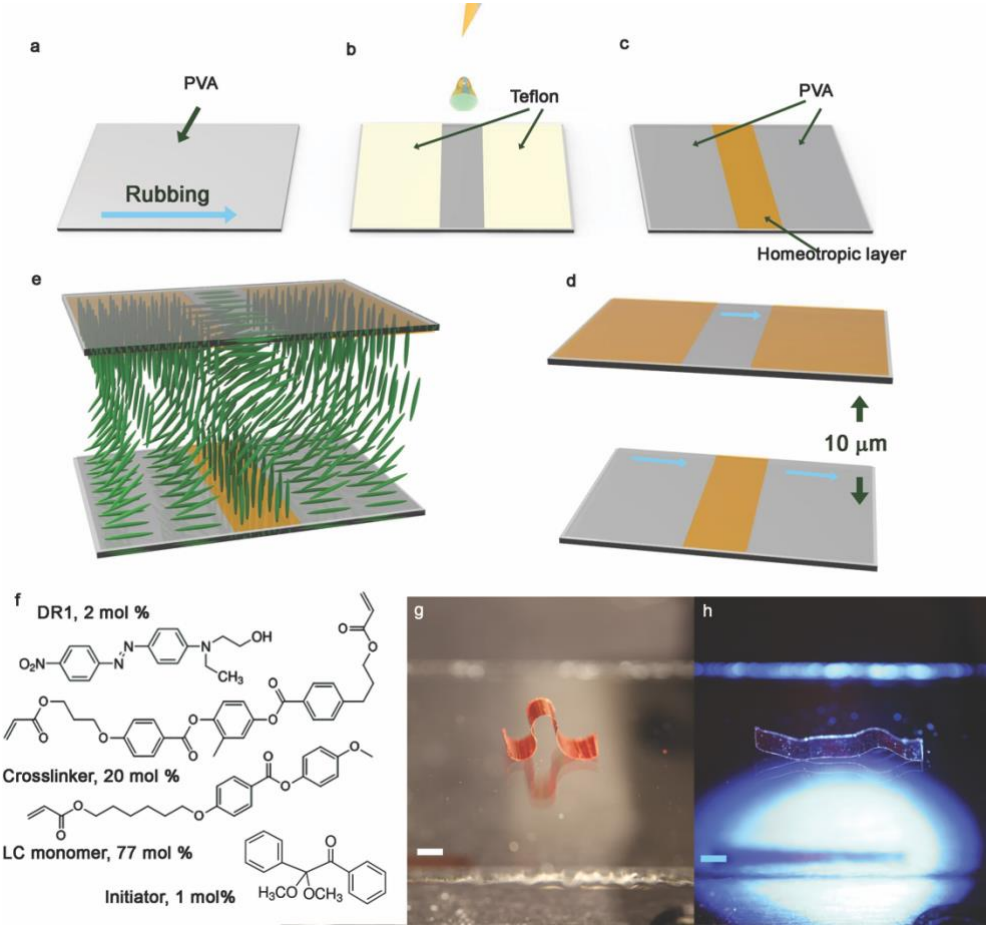

Figure 3. **Photoactuation of the LCE soft microrobot. (**a) Body length change upon different illumination intensities. Error bars indicate the standard deviation obtained from 3 independent measurements. Insets: photographs of the soft robot under different excitation intensities. Scale bars: 2 mm. (b) The photoactuation speed of the inching robot under light excitation with different intensities. Inset: the relaxation speed when the light is turned off.

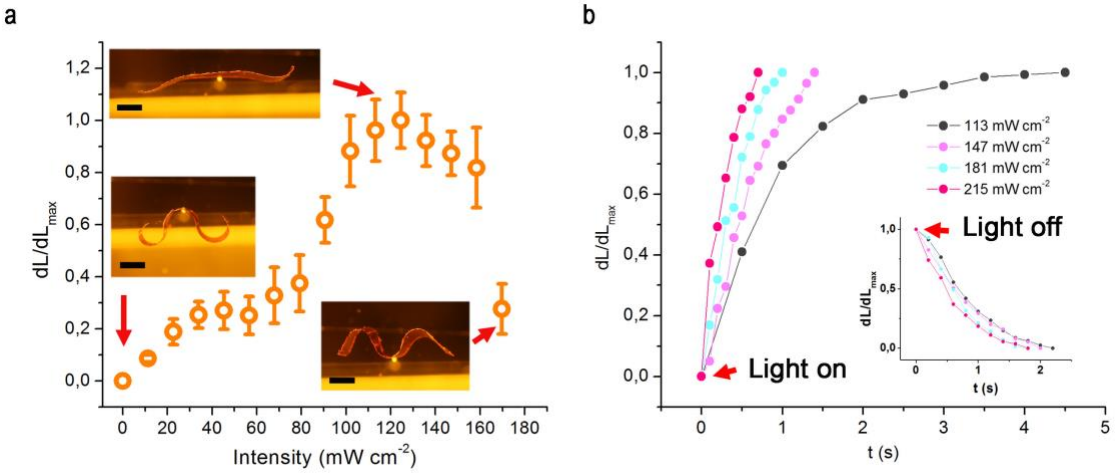

Figure 4. **Light-driven inching locomotion**. Inching motion on (a) paper surface, and (b) on a blazed grating. Inset shows the grating surface topology. (c) Walking distance *vs*. time on the grating and paper surface. Statistics of step lengths on (d) grating surface, and (e) paper surface. The dash lines are Gaussian fits, indicating normal distributions. (f) Light-driven motion on the nail of a human finger. Light source: 488 nm, chopping frequency 0.5 Hz. Intensity: 150 mW cm^{-2} for (a) and (b), 200 mW cm^{-2} for (f). Scale bars: 5 mm. An optical filter is used to block wavelengths below 500 nm in all the images.

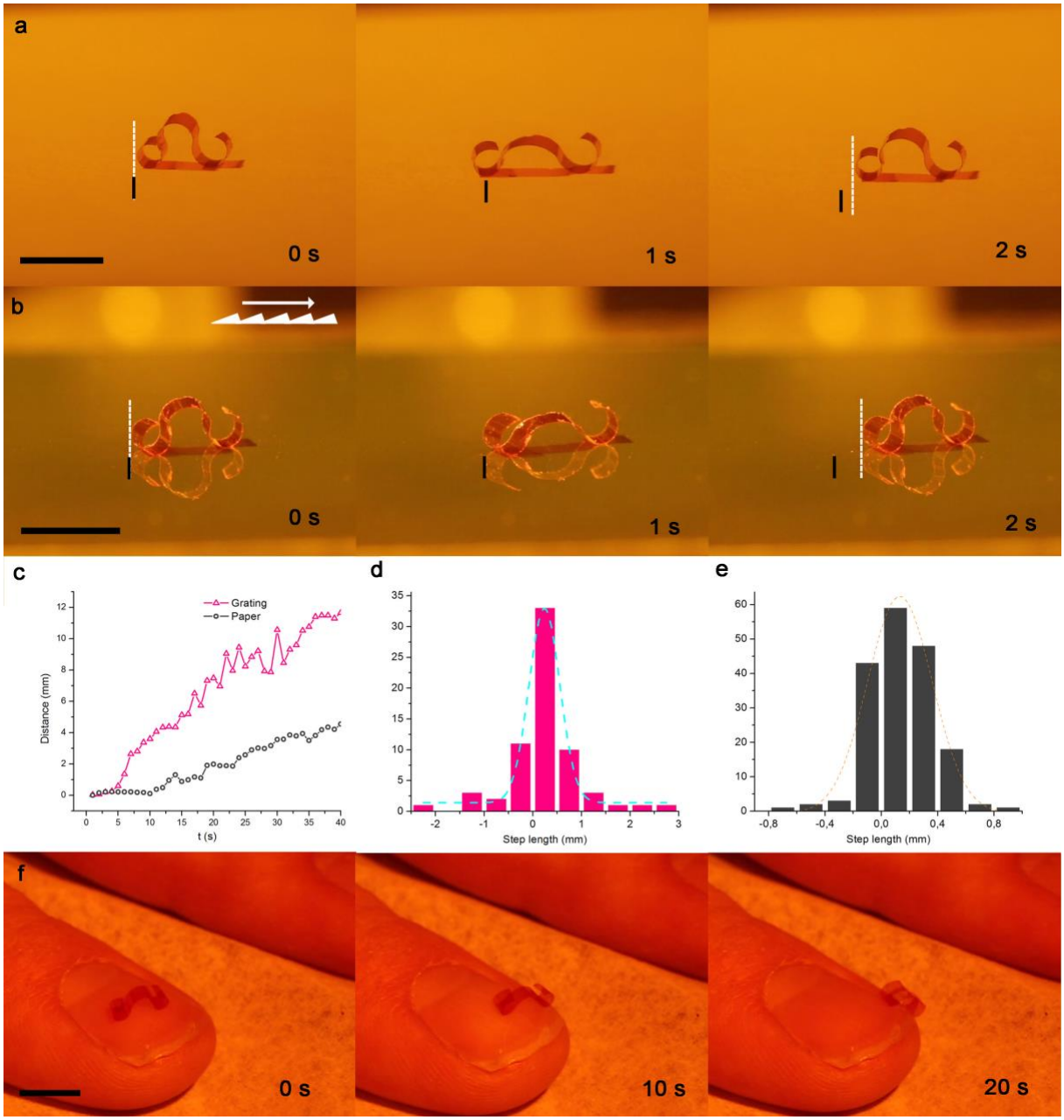

The table of contents entry

Soft robotics brings revolutionary possibilities to devising new moving mechanisms, attracting great attention from both fundamental scientific and application points of view. We report a light-driven, human-friendly microrobot that can mimic caterpillar inching locomotion with spatially uniform illumination. The robot is made of liquid crystal elastomer film with engineered molecular alignment distribution, and it can perform inching gait on various surfaces, including human skin.

Hao Zeng*, Owies M. Wani, Piotr Wasylczyk, Arri Priimagi*

Light-driven, caterpillar-inspired miniature inching robot

ToC figure: